Biotechnology for Biofuels and Bioproducts

RESEARCH

Open Access

Unveiling the underlying molecular mechanisms of high lutein production efficiency in *Chlorella sorokiniana* FZU60 under a mixotrophy/photoautotrophy two-stage strategy by transcriptomic, physiological, and biochemical analyses

Ruijuan Ma[1,2,3,4†], Zhen Zhang[1,2,3,4†], Hong Fang[1,2,3,4], Xinyu Liu[1,2,3,4], Shih-Hsin Ho[3,5], Youping Xie[1,2,3,4*] and Jianfeng Chen[1,2,3,4*]

Abstract

Background *Chlorella sorokiniana* FZU60 is a promising lutein producing microalga. A mixotrophy/photoautotrophy two-stage strategy can achieve high biomass concentration at stage 1 and high lutein content at stage 2, leading to excellent lutein production efficiency in *C. sorokiniana* FZU60. However, the underlying molecular mechanisms are still unclear, restraining the further improvement of lutein production.

Results In this study, physiological and biochemical analysis revealed that photochemical parameters (Fv/Fm and NPQ) and photosynthetic pigments contents increased during the shift from mixotrophy to photoautotrophy, indicating that photosynthesis and photoprotection enhanced. Furthermore, transcriptomic analysis revealed that the glyoxylate cycle and TCA cycle were suppressed after the shift to photoautotrophy, leading to a decreased cell growth rate. However, the gene expression levels of photosynthesis, CO_2 fixation, autophagy, and lutein biosynthesis were upregulated at the photoautotrophy stage, demonstrating that microalgal cells could obtain more precursor to synthesize lutein for enhancing photosynthesis and reducing reactive oxygen species.

Conclusions The findings help to elucidate the molecular mechanisms for high lutein production efficiency of *C. sorokiniana* FZU60 under the mixotrophy/photoautotrophy strategy, identify key functional genes responsible for lutein biosynthesis, and shed light on further improvement of lutein production by genetic or metabolic engineering in future studies.

Keywords *Chlorella sorokiniana* FZU60, Lutein, Mixotrophy, Photoautotrophy, Molecular mechanisms

†Ruijuan Ma and Zhen Zhang contributed equally to this work

*Correspondence:
Youping Xie
ypxie@fzu.edu.cn
Jianfeng Chen
jfchen@fzu.edu.cn
Full list of author information is available at the end of the article

Introduction

Lutein, a primary xanthophyll carotenoid, has many beneficial effects on human health, such as protection of ocular health, anti-inflammatory, beneficial effects in the development of infant brain, and inhibition of adipogenesis [1]. Thus, it has been widely used in food additives, cosmetics, and drugs [2]. The lutein market was valued at USD 135 million in 2015 and is expected to have an annual growth rate of 6% by 2024 [1]. Marigold flowers are the traditional lutein source, while lutein production from them has the disadvantages of high labor intensity, low lutein content, occupation of arable land, and susceptible to climate [3]. In recent years, microalgae have been considered an alternative lutein source due to the advantages of a fast growth rate, high lutein production, and independence of arable land and fresh water resources [2, 4].

The production of microalgae-based lutein can be manipulated in photoautotrophic, mixotrophic, and heterotrophic modes [1, 5]. Among them, photoautotrophy and mixotrophy involve CO_2 fixation [6], and thus are relatively cost-effective if flue gas is used as the CO_2 source [7]. To date, photoautotrophy is the most widely used cultivation mode for microalgae as it is easy to operate and enables the utilization of freely available sunlight [8]. Besides, the biosynthesis of light-induced lutein enhances under this cultivation mode [9]. However, photoautotrophy is limited by light penetration due to the self-shading effects of microalgal cells when cell density increases, leading to a low biomass production [10]. Microalgae cultivated in mixotrophic mode can use both inorganic and organic carbon sources for photosynthesis and aerobic respiration; therefore, the cell growth rate is much higher than that of photoautotrophic mode [11]. However, lutein biosynthesis reduces under the mixotrophic mode [12]. Based on these phenomena, a two-stage strategy with semi-batch mixotrophic cultivation in stage 1 and photoautotrophic induction in stage 2 was explored to initially improve cell growth and then induce lutein accumulation in *Chlorella sorokiniana* MB-1, achieving a high lutein productivity of 7.62 mg/L/d [13]. Likewise, a multi-operation integrated strategy with semi-batch and fed-batch mixotrophic cultivation in stage 1 and photoinduction in stage 2 was applied in *C. sorokiniana* FZU60 to achieve an excellent lutein content, productivity, and production of 9.57 mg/g, 11.57 mg/L/d, and 17.35 mg/L, respectively [9]. Moreover, the mixotrophy/photoautotrophy two-stage strategy could be scaled in a 50 L column photobioreactor in *C. sorokiniana* FZU60 [12]. Nevertheless, the molecular mechanisms for high lutein production efficiency under the mixotrophy/photoautotrophy two-stage strategy have not been elucidated.

Microalgal lutein is connected to light-harvesting complexes (LHCs), presented as a "structural form" for light-harvesting; besides, it functions to dissipate excess light energy for protecting microalgae from photo-oxidative damage by non-photochemical quenching [14, 15]. Hence, the accumulation of lutein is highly associated with photosynthesis. It was found that photosynthesis was shut off by reducing the expression of photosynthetic apparatus protein, including core proteins D2 and CP43 of photosystem II (PSII), core protein PsaA of photosystem I (PSI), and large subunit cytochrome b_6 of the cytochrome b_6f (Cyt b_6f) complex, when the microalga *Chromochloris zofingiensis* was transferred from photoautotrophic to mixotrophic cultivation [16]. In addition, the transcriptional level analysis showed that non-photochemical quenching and photorespiration of *C. zofingiensis* were significantly decreased under mixotrophic condition, compared with that under photoautotrophic condition [17]. Thus, the shift from mixotrophy to photoautotrophy may enhance photosynthesis and photoprotection, resulting in an increase in lutein accumulation due to its functions in light-harvesting and non-photochemical quenching. However, the underlying molecular mechanisms need to be studied.

The present study investigated the growth, physiological, and biochemical parameters of *C. sorokiniana* FZU60 under the mixotrophy/photoautotrophy two-stage strategy. Furthermore, transcriptomic analysis was used to reveal the features of photosynthesis, carbon fixation, autophagy, and lutein biosynthesis under this trophic transition. The findings shed light on the molecular mechanisms for high lutein production efficiency of *C. sorokiniana* FZU60 under the mixotrophy/photoautotrophy strategy and will provide a foundation for future studies on further improvement of lutein production by genetic or metabolic engineering.

Results and discussion

Changes in growth, lutein accumulation, and photochemical parameters under the mixotrophy/photoautotrophy two-stage strategy

As shown in Fig. 1a, biomass concentration raised rapidly from -24 to 0 h, when acetate was replete (Fig. 1b). Then, the growth rate decreased after acetate was depleted (0–72 h). Consistently, nitrate was consumed quickly from -24 to 0 h, and then the consumption rate decreased from 0 to 72 h (Fig. 1c). Hence, microalgal cells grew faster under mixotrophic condition, compared with that under photoautotrophic condition. This result is similar to the studies in *C. zofingiensis*[16], *C. sorokiniana* MB-1 [13], and *Scenedesmus obliquus* KGE-17 [18]. The higher

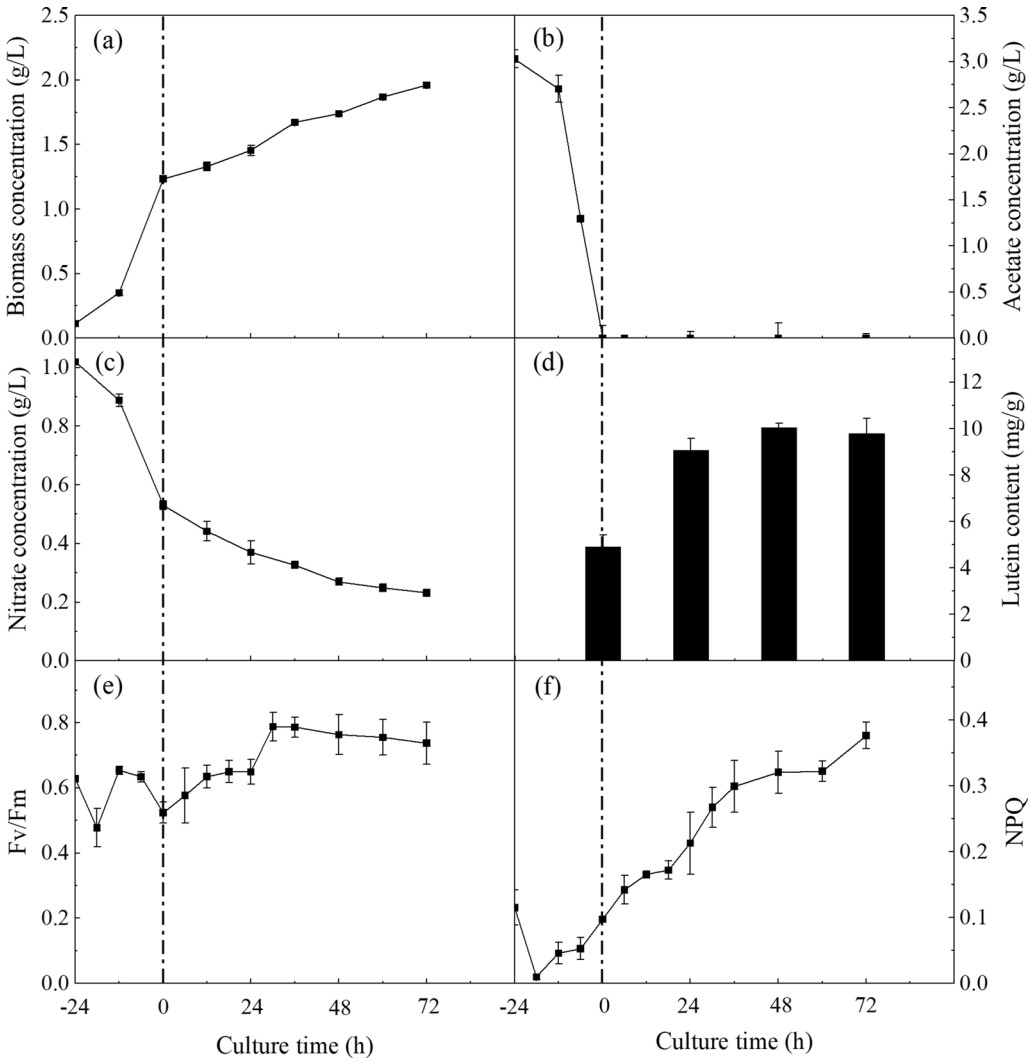

Fig. 1 Time-course profiles of growth, lutein accumulation, and photochemical parameters of *C. sorokiniana* FZU60 under the mixotrophy/photoautotrophy strategy. **a** Biomass concentration; **b** Acetate concentration; **c** Nitrate concentration; **d** Lutein content; **e** Fv/Fm; **f** NPQ. The culture time at the onset of acetate depletion was denoted as 0 h

growth rate under mixotrophic condition might be due to the fact that microalgal cells could simultaneously utilize inorganic and organic carbon sources under lighting condition for photosynthesis and aerobic respiration [11].

On the other hand, lutein content raised significantly from 0 to 48 h, and then plateaued at 72 h (Fig. 1d), indicating that photoautotrophy can stimulate lutein accumulation. Lutein accumulation is highly associated with photosynthesis due to its function in light-harvesting and photoprotection [14, 15]. Hence, the photochemical parameters of Fv/Fm and NPQ representing photosynthesis performance were analyzed. As shown in Fig. 1e, the value of Fv/Fm fluctuated from -24 to 0 h, and then gradually increased from 0 to 30 h. The increase in Fv/Fm value during the shift from mixotrophic to photoautotrophic conditions indicated that the photosynthetic capacity improved [19]. Besides, the value of NPQ decreased initially, followed by a steady increase under mixotrophic condition, and then continuously increased after the transfer to photoautotrophic condition (Fig. 1f). The sharp increase in NPQ value under photoautotrophic condition revealed that the dissipation of light energy increased, which could be a result of the microalgal photoprotection mechanism [20]. Hence, the shift from photoautotrophy to mixotrophy improved photosynthetic capacity and photoprotection, leading to an increase in lutein accumulation.

Variations of biochemical and pigmental compositions under the mixotrophy/photoautotrophy two-stage strategy

Biochemical compositions reveal the physical metabolism of microalgal cells. Thus, the variations in biochemical compositions of *C. sorokiniana* FZU60 under the mixotrophy/photoautotrophy strategy were investigated. As shown in Fig. 2a, the cellular composition consisted mainly of protein, carbohydrate, fatty acid, carotenoid, and chlorophyll. Protein was the major component of microalgal cells. Its content decreased at 0 h, and then increased at 12 and 24 h. The changing trend of carbohydrate content was opposite to protein content, which increased at 0 h, and then declined at 12 and 24 h. No significant difference was observed in fatty acid content. Protein is a primary metabolite, which is accumulated under the optimal conditions for cell growth, while carbohydrate is classified into structural and storage types, the latter of which (such as starch) is largely accumulated under stressed conditions as short-term energy reserve [21]. An increase in carbohydrate content, especially starch content, under stressed conditions has been observed in many microalgae, such as *Chlorella* species [22] and *Neochloris oleoabundans* HK-129 [23]. Thus, the sudden increase in carbohydrate content and decrease in protein content at the onset of acetate depletion indicated that the shift from mixotrophy to photoautotrophy might course transient stress to microalgal cells. Subsequently, carbohydrate content decreased, and protein content increased, when microalgal cells adjusted to the photoautotrophic condition.

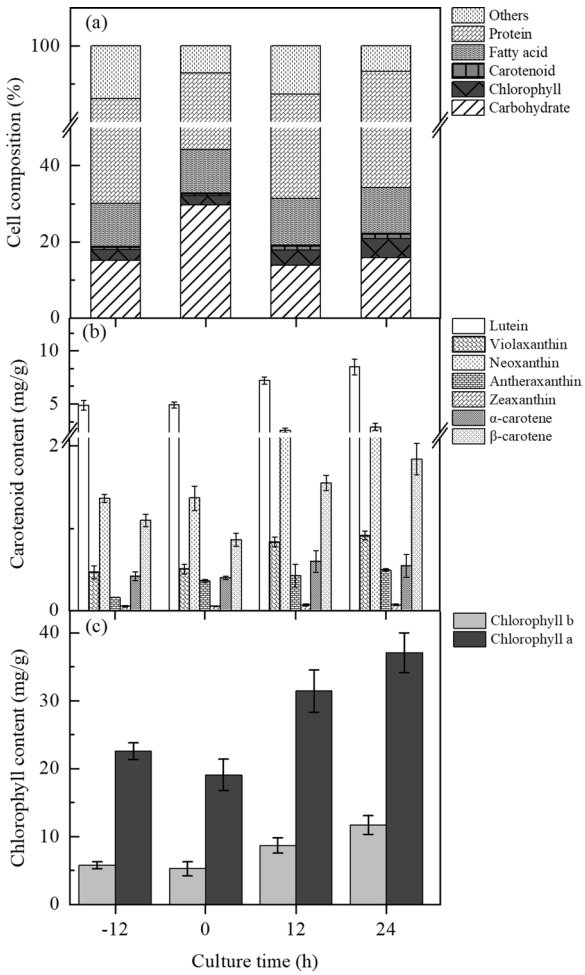

Fig. 2 Time-course profiles of biochemical (**a**), carotenoid (**b**), and chlorophyll (**c**) compositions of *C. sorokiniana* FZU60 under the mixotrophy/photoautotrophy strategy. The culture time at the onset of acetate depletion was denoted as 0 h

The contents of pigments (including carotenoid and chlorophyll) were not significantly different from − 12 to 0 h, while their contents increased sharply from 0 to 24 h (Fig. 2a). It can be observed explicitly in Fig. 2b that the contents of carotenoids, including lutein, violaxanthin, neoxanthin, antheraxanthin, zeaxanthin, α-carotene, and β-carotene, significantly enhanced after microalgal cells were shifted to photoautotrophic condition. Similarly, the contents of chlorophylls, including chlorophyll a and b, significantly increased under photoautotrophic condition (Fig. 2c). Both carotenoid and chlorophyll are photosynthetic pigments [24]. The capture of light by PSII was achieved by a macromolecular complex consisting of major pigments (chlorophyll a and b) and minor pigments (carotenoids of lutein, neoxanthin, and violaxanthin) [25]. The significant increase in their contents indicated that photosynthesis might be greatly enhanced during the shift from mixotrophy to photoautotrophy.

Global gene response at the transcriptional level during the shift from mixotrophy to photoautotrophy

To further investigate the underlying molecular mechanisms of high lutein production efficiency in *C. sorokiniana* FZU60 under the mixotrophy/photoautotrophy two-stage strategy, a transcriptomic analysis was performed based on de novo assembly methods. The obtained unigenes mainly distributed between 150 and 1000 bp (Additional file 1: Fig. S1a). The annotation results indicated that there were 14,677 unigenes annotated in all four databases of KEGG, KOG, Nr, and Swissprot (Fig. 3a). According to the results of Nr annotation, the unigenes were most aligned to *C. sorokiniana* (10,616 unigenes) (Additional file 1: Fig. S1b), confirming that the newly isolated microalga is a species of *C. sorokiniana*. The principal component analysis demonstrated that all transcriptomes were highly corelated with each other within each group (Fig. 3b). DEGs analysis showed that the number of DEGs was distinct between treatment groups (Additional file 1: Fig. S2). Compared with F-12 h

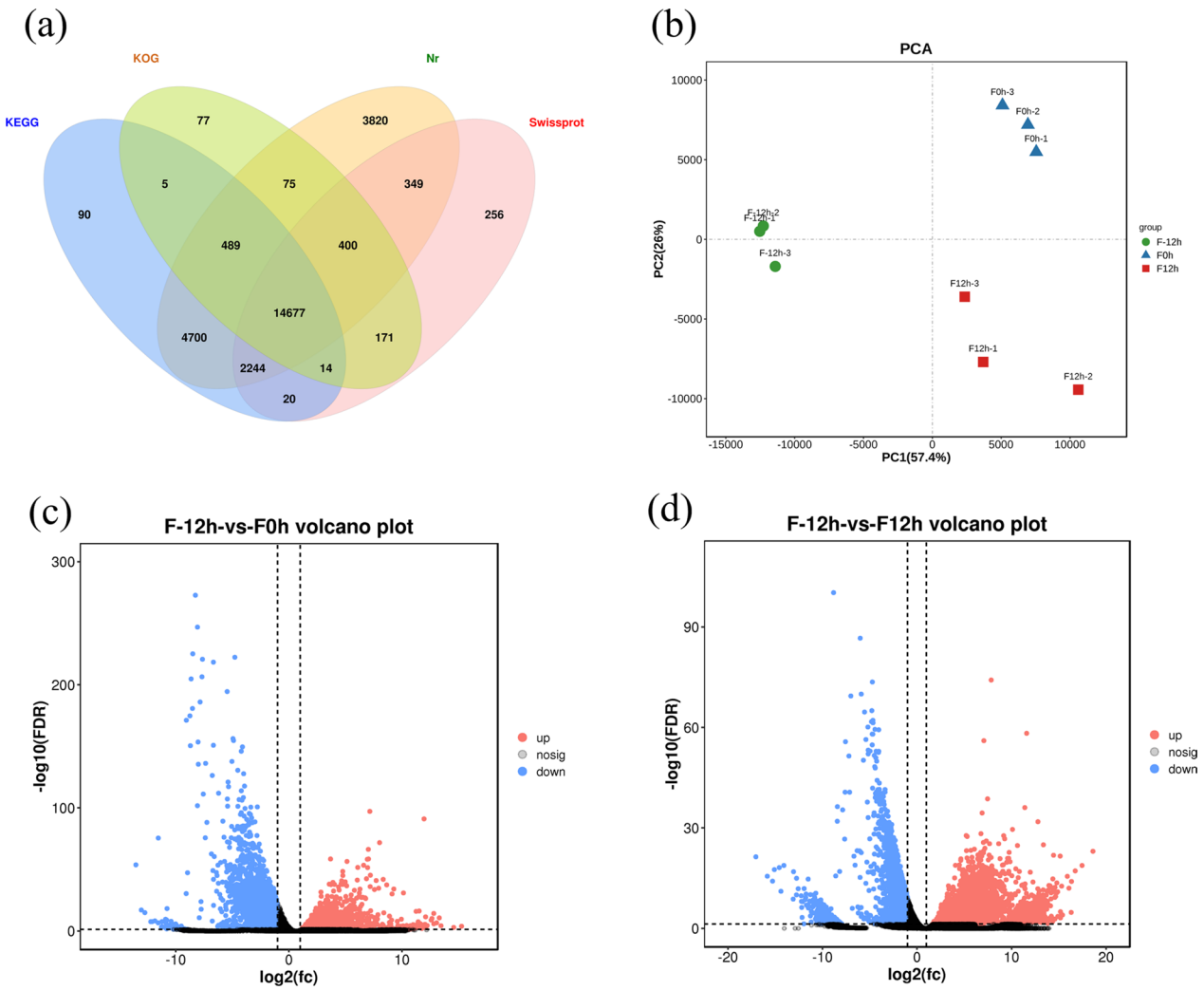

Fig. 3 Global analysis of transcriptomes and DEGs. **a** Venn diagram of annotation results in four databases; **b** Score plot of principle component analysis; **c** Volcano plot of changes in gene expression between F-12 h and F0h groups; **d** Volcano plot of changes in gene expression between F-12 h and F12h groups

group, there was 2323 unigenes were upregulated and 2254 unigenes were downregulated for F0h group (Fig. 3c and Additional file 1: Fig. S2); besides, 12,267 unigenes were upregulated and 2287 unigenes were downregulated for F12h group (Fig. 3d and Additional file 1: Fig. S2). Moreover, the unigenes involved in the pathways of acetate metabolism, photosynthesis, CO_2 fixation, autophagy, and carotenoid biosynthesis were manually identified and their dynamic changes in transcriptional levels were analyzed.

Suppression of glyoxylate cycle and TCA cycle during the shift from mixotrophy to photoautotrophy

Acetate is the organic carbon source used by microalgal cells at the mixotrophy stage, and it was exhausted at the photoautotrophy stage. Thus, the metabolism of acetate might be changed completely during the shift from mixotrophy to photoautotrophy. After uptake in microalgae, acetate is converted into acetyl-CoA at the action of ACS [26]. Results of the transcriptomic analysis showed that the expression level of *ACS* gene was significantly downregulated after acetate was depleted (Fig. 4), indicating that acetate metabolism was sharply suppressed. This result is consistent with the findings in *Chlamydomonas reinhardtii* that the expression level of *ACS* gene was significantly upregulated when microalgal cells were shifted from autotrophic to mixotrophic conditions [27].

Acetate can enter the glyoxylate cycle or TCA cycle, which exists in glyoxysome and mitochondria, respectively [28, 29]. The glyoxylate cycle and TCA cycle share

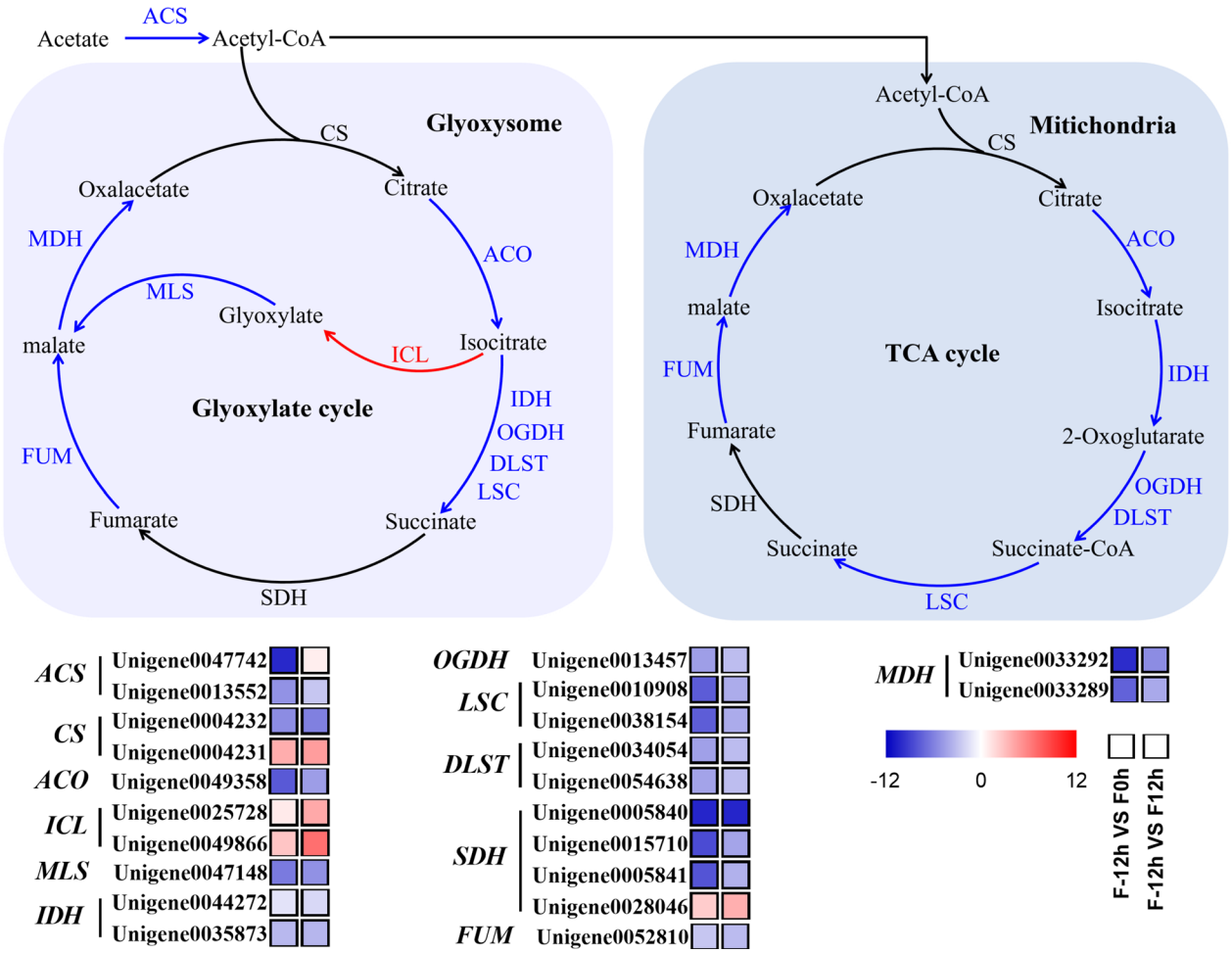

Fig. 4 Transcriptional response of glyoxylate cycle and TCA cycle of *C. sorokiniana* FZU60 under the mixotrophy/photoautotrophy strategy. ACO: aconitate hydratase; ACS: acetyl-CoA synthetase; CS: citrate synthase; DLST: dihydrolipoamide succinyltransferase; FUM: fumarate hydratase; ICL: isocitrate lyase; IDH: isocitrate dehydrogenase; LSC: succinyl-CoA synthetase; MDH: malate dehydrogenase; MLS: malate synthase; OGDH: 2-oxoglutarate dehydrogenase; SDH: succinate dehydrogenase. The red, blue, and black arrows indicate the upregulation, downregulation, and invariability of gene, respectively

similar enzymes, except for two special enzymes (MLS and ICL) in the glyoxylate cycle [28]. As shown in Fig. 4, the expression levels of *ACO*, *IDH*, *OGDH*, *DLST*, *LSC*, *FUM*, and *MDH* genes, presenting in both the glyoxylate cycle and TCA cycle, were significantly downregulated. Besides, the expression levels of *ICL* and *MLS* genes, existing in the glyoxylate cycle, were upregulated and downregulated, respectively. Hence, the transcriptomic analysis showed that most genes in the glyoxylate cycle and TCA cycle were downregulated, indicating that these two pathways were suppressed. The glyoxylate cycle or TCA cycle can provide carbon skeletons and energy (ATP and NADPH) for microalgal cells, which are important for cell growth [30]. Hence, the decrease in cell growth rate during the shift from mixotrophy to photoautotrophy (Fig. 1a) could be due to the suppression of glyoxylate cycle and TCA cycle.

Enhancement of photosynthesis and CO_2 fixation during the shift from mixotrophy to photoautotrophy

Since photosynthesis and CO_2 fixation are closely related to lutein biosynthesis, the changes of them in transcriptomic level were investigated in this study. Photosynthetic apparatus mainly consists of five complexes, including PS I, PS II, Cyt b_6f complex, photosynthetic electron transport, and F-type ATPase [31]. As shown in Fig. 5a, the expression levels of *PsbO* gene in PSII, *PetC* gene in Cyt b_6f complex, as well as *gamma*, *delta*, and *a* genes in F-type ATPase were significantly upregulated at 0 and 12 h. In addition, the expression of *Lhca1*, *Lhcb1* (Unigene0032698), and *Lhcb2* genes in LHCs were upregulated after the shift to photoautotrophy. Lutein is combined with LHCs and functions in light-harvesting and photoprotection [14, 15]. The enhanced gene expression of PSII and LHCs indicated that photosynthesis

increased, which might require more lutein and thus stimulated lutein accumulation. Besides, F-type ATPase is responsible for the generation of energy molecule ATP using H^+ produced by the PS II and Cyt b_6f complex [32]. The increase in gene expression of the F-type ATPase and Cyt b_6f complex indicated that the ATP synthesis enhanced, which could be used as energy for CO_2 fixation and carotenoid accumulation. Hence, the upregulation of genes coding photosynthetic apparatus was in line with the increase in Fv/Fm value and the content of photosynthetic pigments.

Similar to some other microalgae, such as *Chromochloris zofingiensis* [31] and *Thalassiosira weissflogii* [33], both the C_4 cycle and Calvin–Benson cycle for CO_2 fixation exist in *C. sorokiniana* FZU60. As shown in Fig. 5b, the expression level of *RBCS* gene in the Calvin–Benson cycle, responsible for fixing CO_2 into glycerate, was significantly upregulated after the shift to photoautotrophy (0 and 12 h). Besides, the expression levels of *SBP*, *TKL*, *RPI*, *PRK*, and *RPE* genes were all upregulated at 0 and 12 h. Meanwhile, the expression level of some isoforms of *GAPDH*, *PGK*, *FBA*, and *FBP* was upregulated at 0 and 12 h. Thus, CO_2 fixation in the Calvin–Benson cycle was significantly enhanced. Glyceraldehyde-3-phosphate, an essential product of the Calvin–Benson cycle, can be converted into pyruvate, which is the substrate for biosynthesizing the precursor (IPP) of carotenoid [21, 31]. Therefore, the enhanced Calvin–Benson cycle might help to provide more precursor for carotenoid accumulation.

On the other hand, the expression level of *ppc* gene in the C_4 cycle pathway, responsible for the fixation of CO_2 to oxaloacetate, was upregulated at 0 h (Fig. 5b). Besides, the expression level of *NADP-MDH* gene was significantly enhanced after the switch to photoautotrophy (0 and 12 h). The NADP-MDH catalyzes oxaloacetate into malate, which is further transformed into pyruvate, the initial metabolite of the MEP pathway for biosynthesizing the precursor (IPP) of carotenoid [21, 31]. Besides, the expression level of *PPDK* gene, responsible for catalyzing pyruvate into phosphoenol-pyruvate, was downregulated after the shift to photoautotrophy (0 and 12 h). Hence, the biosynthesis of pyruvate from oxaloacetate and malate increased, while the transformation of pyruvate into phosphoenol-pyruvate decreased, which could facilitate pyruvate accumulation and thus enhance carotenoid biosynthesis.

Enhancement of autophagy during the shift from mixotrophy to photoautotrophy

Autophagy is the main degradation pathway for recycling cellular waste components in microalgal cells, which is activated under stressed conditions, such as oxidative stress [34, 35]. It has been found that carotenoid biosynthesis and autophagy genesis are induced simultaneously to reduce reactive oxygen species (ROS), thus providing a defense against photo-oxidative damage [36]. The increase in NPQ value after the shift to photoautotrophy (Fig. 1f) indicated that the dissipation of light energy increased, which was used for the defense against photo-oxidative damage [20]. Hence, the shift from mixotrophy to photoautotrophy might result in an increase in ROS level and photo-oxidative damage to microalgal cells, thus enhancing carotenoid biosynthesis and autophagy genesis.

The autophagy machinery consists mainly of the ATG1 initiation complex, PI3K nucleation complex, PI3P binding complex, ATG8 ubiquitin-like system, and ATG12 ubiquitin-like system [37]. As shown in Fig. 6, the expression levels of *ATG1* gene in the ATG1 initiation complex, *ATG6*, *VPS15*, and *VPS34* genes in the PI3K nucleation complex, *ATG9* and *ATG18* genes in the PI3P binding complex, *ATG3*, *ATG4*, *ATG7*, and *ATG8* genes in the ATG8 ubiquitin-like system, as well as *ATG10* gene in the ATG12 ubiquitin-like system were all upregulated after the shift to photoautotrophy (0 and 12 h). To be noted, ATG8 protein is vital for the formation and maturation of autophagosome, a double membrane vesicle that engulfs cytosolic components [38]. The results showed that all five isoforms of *ATG8* gene were significantly upregulated. Thus, autophagy was strongly activated in *C. sorokiniana* FZU60 after the shift to photoautotrophy, indicating that ROS level might increase in microalgal cells, which could induce carotenoid biosynthesis simultaneously [36].

(See figure on next page.)

Fig. 5 Transcriptional response of photosynthesis **a** and CO_2 fixation **b** of *C. sorokiniana* FZU60 under the mixotrophy/photoautotrophy strategy. a: F-type H^+-transporting ATPase subunit a; delta: F-type H + -transporting ATPase subunit delta; FBA: fructose-bisphosphate aldolase; FBP: fructose-1,6-bisphosphatase I; gamma: F-type H^+-transporting ATPase subunit gamma; GAPDH: glyceraldehyde 3-phosphate dehydrogenase; Lhca1: light-harvesting complex I chlorophyll a/b binding protein 1; Lhca2: light-harvesting complex I chlorophyll a/b binding protein 2; Lhcb1: light-harvesting complex II chlorophyll a/b binding protein 1; Lhcb2: light-harvesting complex II chlorophyll a/b binding protein 2; ME: malic enzyme; NADP-MDH: chloroplast NADP-malate dehydrogenase; PetC: cytochrome b_6f complex iron-sulfur subunit; PGK: phosphoglycerate kinase; PPC: phosphoenolpyruvate carboxylase; PPDK: pyruvate orthophosphate dikinase; PRK: phosphoribulokinase; PsbO: photosystem II oxygen-evolving enhancer protein 1; RBCS: ribulose-bisphosphate carboxylase; RPE: ribulose-phosphate 3-epimerase; RPI: ribose 5-phosphate isomerase; SBP: sedoheptulose-1,7-bisphosphatase; TKL: transketolase. The red, blue, and black arrows indicate the upregulation, downregulation, and invariability of gene, respectively

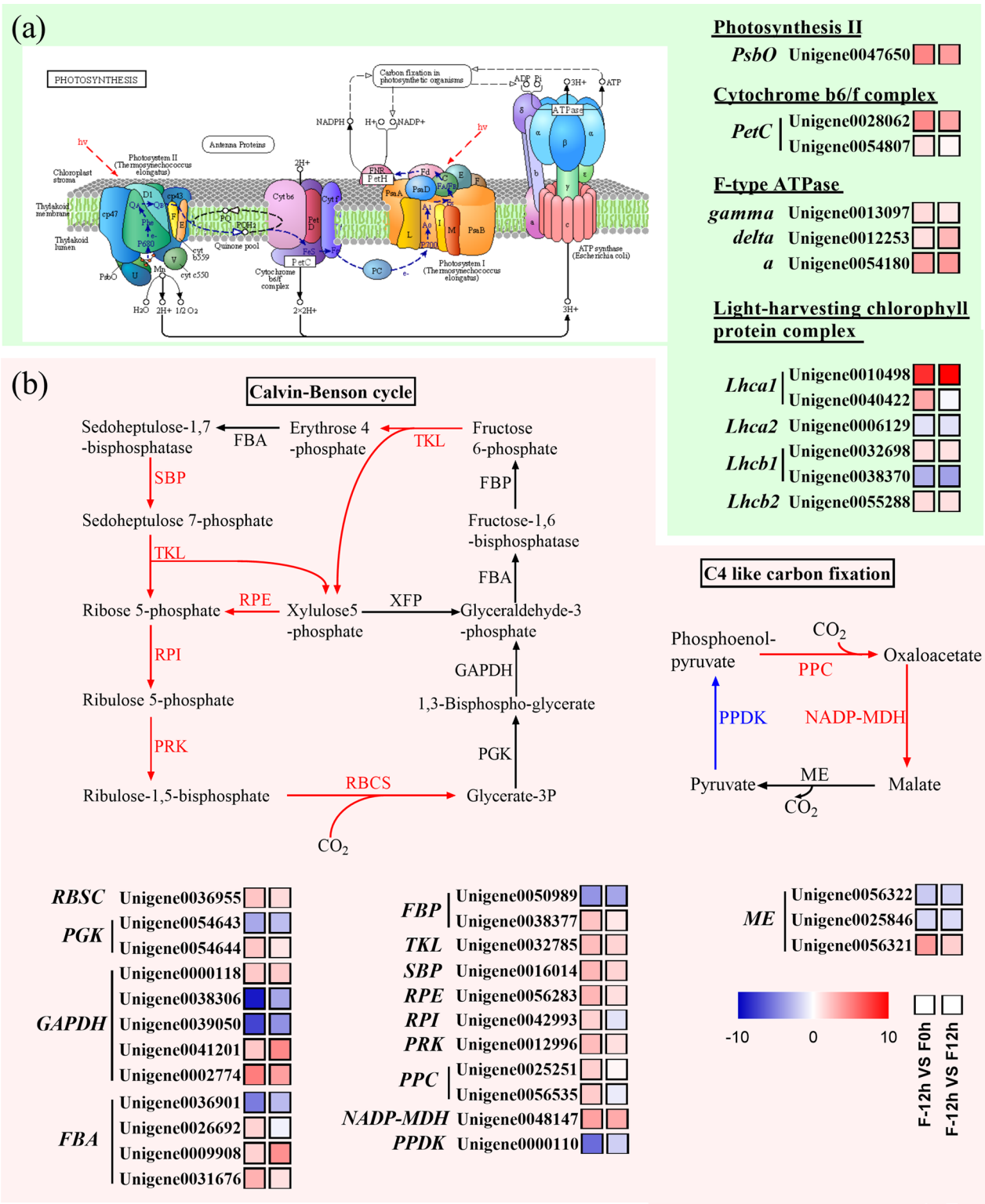

Fig. 5 (See legend on previous page.)

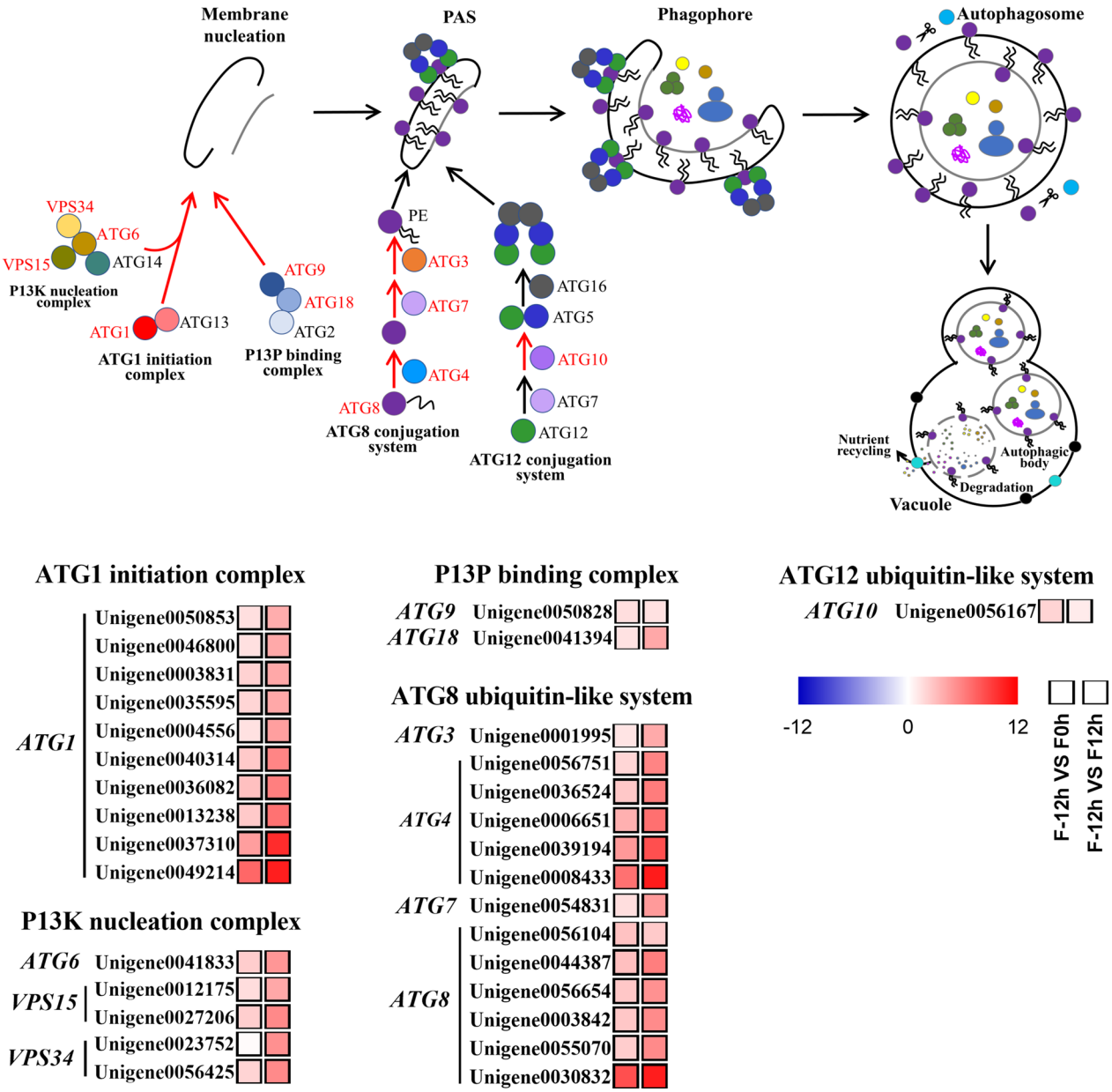

Fig. 6 Transcriptional response of autophagy of *C. sorokiniana FZU60* under the mixotrophy/photoautotrophy strategy. ATG1: autophagy-related protein 1; ATG2: autophagy-related protein 2; ATG3: autophagy-related protein 3; ATG4: autophagy-related protein 4; ATG5: autophagy-related protein 5; ATG6: autophagy-related protein 6; ATG7: autophagy-related protein 7; ATG8: autophagy-related protein 8; ATG9: autophagy-related protein 9; ATG10: autophagy-related protein 10; ATG12: autophagy-related protein 12; ATG13: autophagy-related protein 13; ATG18: autophagy-related protein 18; VPS15: phosphoinositide-3-kinase; VPS34: phosphatidylinositol 3-kinase. The red, blue, and black arrows indicate the upregulation, downregulation, and invariability of gene, respectively

Enhancement of lutein biosynthesis during the shift from mixotrophy to photoautotrophy

Lutein biosynthesis initiates from IPP and its isomer DMAPP, which are biosynthesized by the MEP pathway [1]. The product GGPP is converted into phytoene at the catalyzation of PSY [39]. Phytoene is transformed into ζ-carotene by PDS and then lycopene by ZDS, Z-ISO, and CRTISO [40]. As shown in Fig. 7, the expression levels of *PDS* and *ZDS* genes were significantly upregulated when acetate was depleted (0 h), which could lead to an enhanced accumulation of lycopene, a precursor of carotenoid, thus enhancing carotenoid biosynthesis (Fig. 2a). Studies in *Haematococcus pluvialis* indicated that the expression level of *PDS* gene was upregulated during

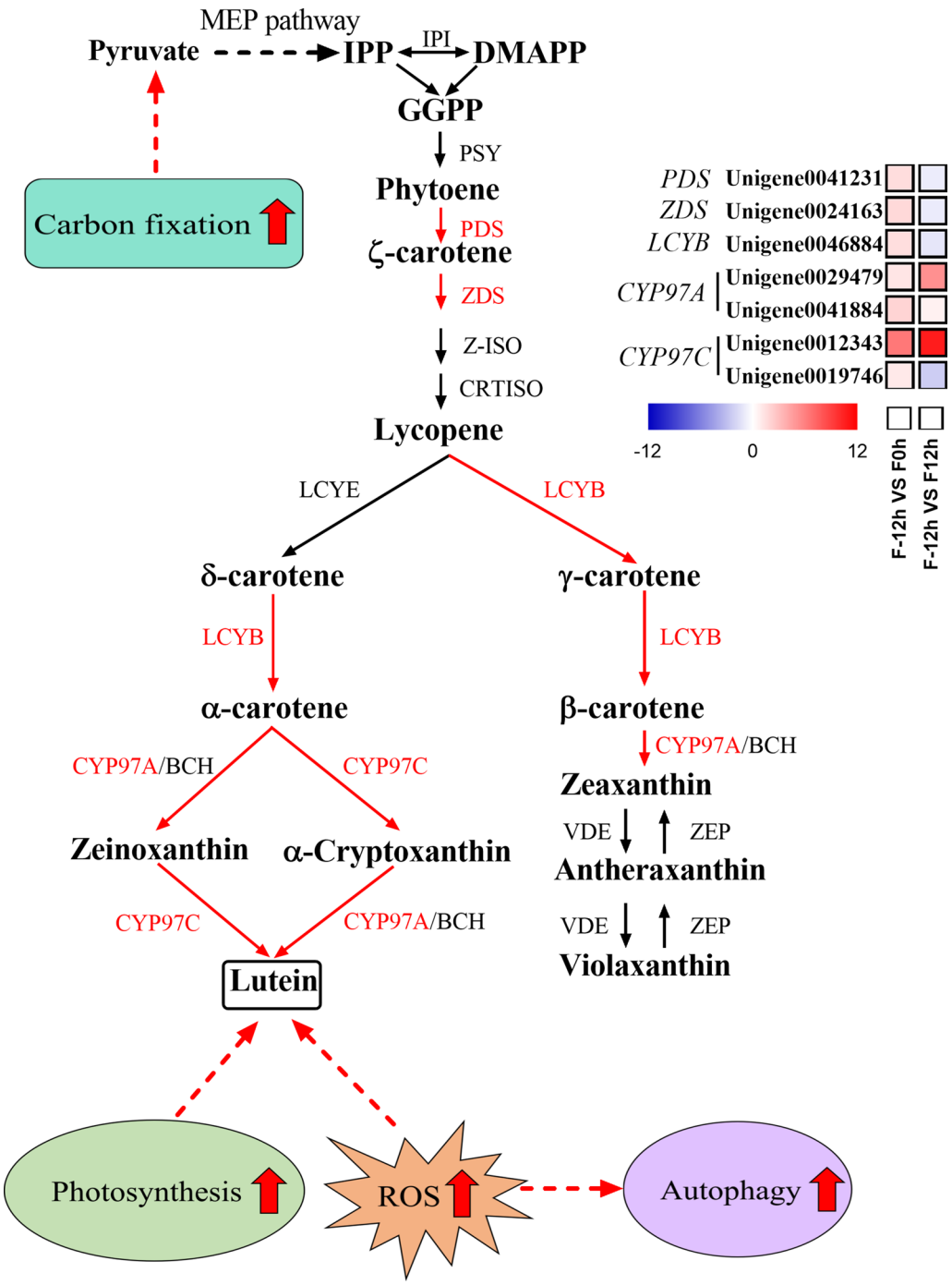

Fig. 7 Transcriptional response of carotenoid biosynthesis of *C. sorokiniana FZU60* under the mixotrophy/photoautotrophy strategy. BCH: β-carotene hydroxylase; CRTISO: prolycopene isomerase; CYP97A: cytochrome P450 carotenoid hydroxylase A; CYP97C: cytochrome P450 carotenoid hydroxylase C; DMAPP: dimethylallyl diphosphate; IPP: isopentenyl diphosphate; LCYB: lycopene beta-cyclase; LCYE: lycopene epsilon-cyclase; PDS: phytoene desaturase; PSY: phytoene synthase; VDE: violaxanthin deepoxidase; ZDS: zeta-carotene desaturase; ZEP: zeaxanthin epoxidase; Z-ISO: zeta-carotene isomerase. The red, blue, and black arrows indicate the upregulation, downregulation, and invariability of gene, respectively

carotenoid accumulation [41], and the overexpression of endogenous *PDS* gene significantly enhanced carotenoid accumulation [42].

Afterward, lycopene subsequently flows into two branches. For one branch, lycopene is catalyzed into δ-carotene and then α-carotene at the action of LCYE and LCYB [43]. Further, α-carotene is transformed into lutein through zeinoxanthin or α-cryptoxanthin at the action of CYP97C and BCH or CYP97A [44]. Results showed that *LCYB* gene was significantly upregulated at 0 h (Fig. 7), which was consistent with the increase in the contents of α-carotene and β-carotene (Fig. 2b). It should be noted that the expression levels of two isoforms of *CYP97A* gene and one isoform of *CYP97C* gene were upregulated at both 0 and 12 h (Fig. 7). CYP97A and CYP97C are important for catalyzing lutein biosynthesis [44]. Hence, the upregulation of *CYP97A* and *CYP97C* genes resulted in an increase in lutein content. For the other branch, lycopene is catalyzed into γ-carotene and then β-carotene by LCYB. Subsequently, β-carotene is converted into zeaxanthin by BCH or CYP97A [44], which is then transformed into antheraxanthin and violaxanthin, consisting of the violaxanthin cycle [45]. The enhanced contents of carotenoids in the violaxanthin cycle, including zeaxanthin, antheraxanthin, and violaxanthin (Fig. 2b), might be due to the upregulation of *LCYB* and *CYP97A* genes (Fig. 7).

Noticeably, the expression levels of *PDS*, *ZDS*, *LCYB* genes, and one isoform of *CYP97C* gene (Unigene0019746) were downregulated at 12 h. It has been found that gene expression generally precedes the biosynthesis of metabolites [31, 46]. Microalgal cells were under photoautotrophic condition from 0 h. Therefore, the upregulation of lutein biosynthesis genes at 0 h might lead to the translation of sufficient enzymes for enhanced lutein accumulation.

Validation of selected genes by qPCR

To validate RNA-seq data, 10 genes were selected to analyze the expression pattern by qPCR. As shown in Fig. 8, the expression levels of *ACS* and *ACO* genes, involved in acetate metabolism, were downregulated at 0 and 12 h compared with that at -12 h. Besides, the expression levels of *PsbO*, *NADP-MDH*, and *VPS34* genes, involved in photosynthesis, CO_2 fixation, and autophagy, were upregulated at 0 and 12 h. Furthermore, the expression levels of some lutein biosynthesis-related genes, including *PDS*, *ZDS*, *LCYB*, and *CYP97C*, were upregulated at 0 h but downregulated at 12 h; however, the expression level of *CYP97A* gene was upregulated at both 0 and 12 h.

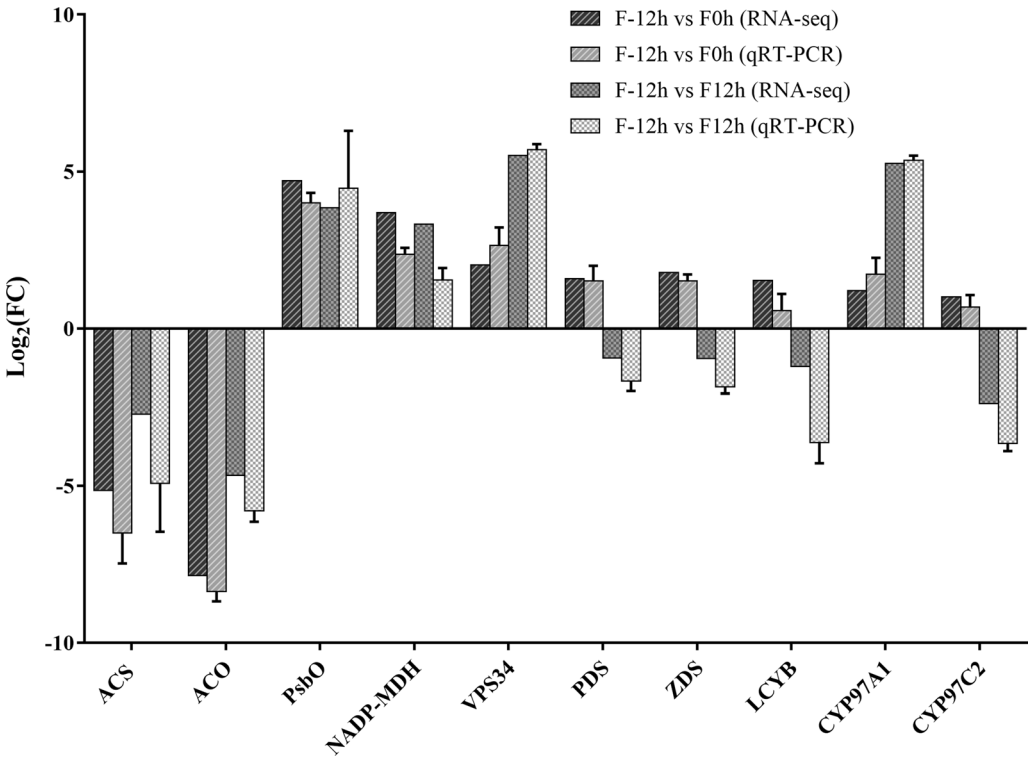

Fig. 8 Expression validation of selected genes by qPCR. The unigene number of selected genes is as follows: *ACS* (Unigene0013552), *ACO* (Unigene0049358), *PsbO* (Unigene0047650), *NADP-MDH* (Unigene0047650), *VPS34* (Unigene0056425), *PDS* (Unigene0041231), *ZDS* (Unigene0024163), *LCYB* (Unigene0046884), *CYP97A* (Unigene0029479), and *CYP97C* (Unigene0019746)

The expression pattern of the abovementioned genes was consistent with that of RNA-seq data. Hence, the RNA-seq data are reliable and accurate.

Conclusions

C. sorokiniana FZU60 grew rapidly at the mixotrophy stage, while lutein accumulation enhanced at the photoautotrophy stage. Based on the physiological, biochemical, and transcriptomic data, the decrease in cell growth after the shift to photoautotrophy could be due to the suppression of glyoxylate cycle and TCA cycle. Besides, the increase in photosynthesis and CO_2 fixation at the photoautotrophy stage could provide more precursor for lutein accumulation. Moreover, the enhancement of autophagy indicated that ROS level might increase, which could induce lutein biosynthesis simultaneously. Hence, the increase in photosynthesis, CO_2 fixation, and ROS level after the shift from mixotrophy to photoautotrophy could trigger lutein biosynthesis (Fig. 7).

Methods

Microalgal strain and culture conditions

C. sorokiniana FZU60 is a newly isolated microalga with high lutein content [9]. The microalgal strain was preserved in a 1.5% (w/v) agar plate with BG11 medium [47].

For pre-culture, microalgal cells were inoculated into a 1-L photobioreactor with BG11 medium at a working volume of 1 L. The microalgal culture was deposited in a light incubator under the conditions of initial pH 7.5, temperature 28 °C, light intensity 250 μmol/m^2/s, and stirring speed 300 r/min. Besides, 2.5% CO_2 was constantly aerated into the microalgal culture. The cultivation lasted 3 days.

The pre-cultured microalgal cells were centrifugated at 5000 r/min, and then inoculated into a 1-L photobioreactor with a working volume of 1 L. The microalgal cells were cultivated with a modified BG11 medium (1 g/L $NaNO_3$) adding 3 g/L CH_3COONa with an inoculation size of 100 mg/L. The change in initial $NaNO_3$ concentration to 1 g/L is due to that the cell growth and lutein accumulation are better at this concentration under mixotrophic cultivation, and nitrogen is still replete after the shift to photoautotrophy, according to our previous study [9]. The cultivation conditions were similar to that of pre-culture except that the temperature was set at 33 °C, which is due to that both cell growth and lutein accumulation are optimal at this temperature [48]. The culture time at the onset of acetate depletion was denoted as 0 h; thus, microalgal cells were cultivated under mixotrophic and photoautotrophic conditions before and after 0 h, respectively. The microalgal culture was collected at set time intervals to analyze biomass concentration, lutein content, chlorophyll fluorescence parameters, biochemical composition, and transcriptome.

Determination of biomass concentration

The optical density of 682 nm (OD_{682}) of microalgal culture was measured by a spectrophotometer (U-2001, Hitachi, Tokyo, Japan). The biomass concentration of microalgal culture was determined by the equation as follows:

$$y = 0.2440x + 0.0156\left(R^2 = 0.9961\right)$$

where y is biomass concentration, and x is OD_{682}.

Determination of acetate and nitrogen concentrations

The microalgal culture was sampled every 12 h and filtered through a 0.22 μm filter. The supernatant was collected and properly diluted to determine the acetate and nitrogen concentrations. The acetate concentration was measured by a total organic carbon analyzer (TOC-L CPH, Shimadzu, Kyoto, Japan), as previously reported [9]. The nitrate concentration was analyzed using a colorimetric method [12].

Chlorophyll fluorescence analysis

The chlorophyll fluorescence of microalgal cells was determined every 12 h from -24 to 36 h and every 24 h from 36 to 72 h. Microalgal culture of 3 mL was sampled in a 5-mL quartz cuvette and kept in the dark for 20 min to reopen PSII reaction centers and relax non-photochemical quenching [19]. The maximum PSII photochemical quantum yield (Fv/Fm) and non-photochemical quenching (NPQ) were determined by a fluorometer (WATER-ED, EDEE0300, Walz, Effeltrich, Germany).

Analysis of biochemical compositions of microalgal cells

The biochemical compositions of microalgal cells were measured at -12, 0, 12, and 24 h. Besides, lutein content was also measured at 48 and 72 h to investigate the changing trend. The determination of carotenoid, chlorophyll, carbohydrate, and fatty acid contents was carried out according to a previous report [49]. A protein extraction kit (BB-3131-1, BestBio, Shanghai, China) was used to extract protein. The protein content was measured by a Pierce® BCA protein assay kit (Thermo Scientific, Waltham, MA, USA).

RNA sequencing (RNA-seq)

The microalgal culture was sampled at − 12, 0, and 12 h with three biological replicates for RNA extraction, when acetate was replete (designated as F-12 h group), at the onset of depletion (designated as F0h group), and

completely depleted (designated as F12 group), respectively. RNA extraction was carried out with a Trizol reagent kit (Invitrogen, Carlsbad, CA, USA), and the RNA quality was examined on an Agilent 2100 bioanalyzer (Agilent Technologies, Palo Alto, CA, USA). The oligo(dT) beads were used to enrich mRNA, which was then fragmented, and reverse transcribed into cDNA with random primers. Subsequently, a QiaQuick PCR extraction kit (Qiagen, Venlo, The Netherlands) was used to purify the cDNA fragments, which were then end repaired, A base added, and linked to Illumina sequencing adapters. Sequencing was carried out by Gene Denovo Biotechnology Co. (Guangzhou, China) utilizing Illumina novaseq 6000.

Sequence assembly and annotation

The raw reads were filtered by fastp (version 0.18.0), and the reads containing adapters, ploy-N, and more than 50% of low-quality bases were removed. The reads were then assembled using Trinity software, and the assembly integrity was assessed by BUSCO. The Unigene sequences were then compared to the protein databases NR, SwissProt, KEGG, and COG/KOG by blastx to obtain the protein with the highest sequence similarity, thus achieving the annotation information of the protein function of Unigene.

Analysis of differentially expressed genes (DEGs)

The DEGs between two distinct groups were analyzed by DESeq2 software [50] and by edgeR [51] between two samples. The genes with the parameters of false discovery rate (FDR) < 0.05 and absolute fold change (FC) ≥ 2 were considered DEGs [52]. The RNA-seq data are shown as $\log_2$ (FC). The data of $\log_2$ (FC) and FDR for the genes analyzed in this study are listed in Additional file 2: Table S1–S4.

Quantitative real-time PCR (qPCR) for validating the expression of selected genes

A total of 10 genes were selected for expression validation, including *ACS* responsible for converting acetate into acetyl-CoA, *ACO* presenting in both the glyoxylate cycle and TCA cycle, *PsbO* presenting in photosynthetic apparatus, *NADP-MDH* involved in CO_2 fixation, *VPS34* involved in autophagy, and *PDS*, *ZDS*, *LCYB*, *CYP97A*, and *CYP97C* involved in lutein biosynthesis. Total RNA of 1 μg was used for cDNA synthesis using EasyScript® First-Strand cDNA Synthesis SuperMix (TransGen Biotech, Beijing, China). The qPCR was carried out by CFX Connect™ Real-Time PCR Detection System (BIO-RAD, Hercules, CA, USA) with SYBR® Premix Ex TaqTM II (TaKaRa, Japan). The program was as follows: an initial denaturation at 95 °C for 30 s; 40 cycles of denaturation at 95 °C for 5 s and annealing/extension at 60 °C for 20 s; a temperature ramping step for producing melting curve at 60 °C for 15 s. The coding gene of ribosomal protein L19 (RPL19) was used as the reference gene, according to a previous study [53]. The $2^{-\Delta Ct}$ method was used to analyze the transcript levels of selected genes based on cycle threshold (Ct) values. All primers are listed in Additional file 2: Table S5.

Statistical analysis

The data of growth, physiological, and biochemical parameters as well as qPCR analysis are shown as average ± standard deviation. Duncan's test of one-way ANOVA analysis was performed to find significant differences ($p < 0.05$) using IBM SPSS Statistics 24.

Abbreviations

Cyt b_6f	Cytochrome b_6f
DEGs	Differentially expressed genes
F-12 h	Samples collected at 12 h before acetate depletion
F0h	Samples collected at the time point of the onset of acetate depletion
F12	Samples collected at 12 h after acetate depletion
FC	Fold change
FDR	False discovery rate
Fv/Fm	The maximum PSII photochemical quantum yield
LHCs	Light-harvesting complexes
NPQ	Non-photochemical quenching
qPCR	Quantitative real-time PCR
RNA-seq	RNA sequencing
ROS	Reactive oxygen species
PSII	Photosystem II
PSI	Photosystem I

Supplementary Information

The online version contains supplementary material available at https://doi.org/10.1186/s13068-023-02300-8.

Additional file 1: Figure S1. The number of unigenes (a) and length distribution of unigenes (b) in *C. sorokiniana* FZU60. **Figure S2**. The numbers of differentially expressed genes among three treatment groups.

Additional file 2: Table S1 RNA-Seq data for the genes involved in glyoxylate cycle and TCA cycle. **Table S2** RNA-Seq data for the genes involved in photosynthesis and CO_2 fixation. **Table S3** RNA-Seq data for the genes involved in autophagy. **Table S4** RNA-Seq data for the genes involved in carotenoid biosynthesis. **Table S5** Primers used for expression validation of selected genes by qRT-PCR.

Acknowledgements

We are grateful to Guangzhou Genedenovo Biotechnology Co., Ltd for assisting in sequencing and bioinformatics analysis.

Author contributions

R.M. and Z.Z. contributed equally to this work. R.M. analyzed the data and wrote the manuscript; Z.Z. performed the experiments and analyzed the data; H.F. performed the experiments; X.L. analyzed the data; S.H.H. modified the language and revised the manuscript; Y.X. designed the research and revised the manuscript; J.C. designed the research. All authors read and approved the final manuscript.

Funding
This study was financially supported by the scientific research project of Fuzhou Institute of Oceanography, China (No. 2022F02), the National Natural Science Foundation of China (No. 32202960), and the Natural Science Foundation of Fujian Province, China (Nos. 2020J01484 and 2021J05127).

Availability of data and materials
All data generated or analyzed during this study are included in this manuscript and its supplementary information files. The raw data of RNA-seq generated in this study have been deposited in the Genome Sequence Archive (accession number: CRA008480) in BIG Data Center (http://bigd.big.ac.cn), Beijing Institute of Genomics (BIG), China Academy of Sciences.

Declarations

Ethics approval and consent to participate
Not applicable.

Consent for publication
Not applicable.

Competing interests
The authors declare that they have no competing interests.

Author details
[1]Marine Biological Manufacturing Center of Fuzhou Institute of Oceanography, Fuzhou University, Fuzhou 350108, China. [2]Technical Innovation Service Platform for High Value and High-Quality Utilization of Marine Organism, Fuzhou University, Fuzhou 350108, China. [3]Fujian Engineering and Technology Research Center for Comprehensive Utilization of Marine Products Waste, Fuzhou University, Fuzhou 350108, China. [4]Fuzhou Industrial Technology Innovation Center for High-Value Utilization of Marine Products, Fuzhou University, Fuzhou 350108, China. [5]State Key Laboratory of Urban Water Resource and Environment, School of Environment, Harbin Institute of Technology, Harbin 150090, China.

Received: 9 December 2022 Accepted: 8 March 2023
Published online: 15 March 2023

References

1. Zheng HS, Wang Y, Li S, Nagarajan D, Varjani S, Lee DJ, Chang JS. Recent advances in lutein production from microalgae. Renew Sust Energ Rev. 2022;153: 111795.
2. Xie YX, Xiong XC, Chen SL. Challenges and potential in increasing lutein content in microalgae. Microorganisms. 2021;9:1068.
3. Lin JH, Lee DJ, Chang JS. Lutein production from biomass: Marigold flowers versus microalgae. Bioresour Technol. 2015;184:421–8.
4. Sun XM, Ren LJ, Zhao QY, Ji XJ, Huang H. Microalgae for the production of lipid and carotenoids: a review with focus on stress regulation and adaptation. Biotechnol Biofuels. 2018;11:272.
5. Sun H, Zhao W, Mao X, Li Y, Wu T, Chen F. High-value biomass from microalgae production platforms: strategies and progress based on carbon metabolism and energy conversion. Biotechnol Biofuels. 2018;11:227.
6. Yang C, Hua Q, Shimizu K. Energetics and carbon metabolism during growth of microalgal cells under photoautotrophic, mixotrophic and cyclic light-autotrophic/dark-heterotrophic conditions. Biochem Eng J. 2000;6:87–102.
7. Molino A, Mehariya S, Iovine A, Casella P, Marino T, Karatza D, Chianese S, Musmarra D. Enhancing biomass and lutein production from *Scenedesmus almeriensis*: effect of carbon dioxide concentration and culture medium reuse. Front Plant Sci. 2020;11:415.
8. Pal P, Chew KW, Yen HW, Lim JW, Lam MK, Show PL. Cultivation of oily microalgae for the production of third-generation biofuels. Sustainability-Basel. 2019;11:5424.
9. Xie Y, Li J, Ma R, Ho SH, Shi X, Liu L, Chen J. Bioprocess operation strategies with mixotrophy/photoinduction to enhance lutein production of microalga *Chlorella sorokiniana* FZU60. Bioresour Technol. 2019;290: 121798.
10. Liyanaarachchi VC, Premaratne M, Ariyadasa TU, Nimarshana PHV, Malik A. Two-stage cultivation of microalgae for production of high-value compounds and biofuels: a review. Algal Res. 2021;57:102353.
11. Chen CY, Ho SH, Liu CC, Chang JS. Enhancing lutein production with *Chlorella sorokiniana* Mb-1 by optimizing acetate and nitrate concentrations under mixotrophic growth. J Taiwan Inst Chem Eng. 2017;79:88–96.
12. Xie Y, Li J, Ho SH, Ma R, Shi X, Liu L, Chen J. Pilot-scale cultivation of *Chlorella sorokiniana* FZU60 with a mixotrophy/photoautotrophy two-stage strategy for efficient lutein production. Bioresour Technol. 2020;314: 123767.
13. Chen CY, Liu CC. Optimization of lutein production with a two-stage mixotrophic cultivation system with *Chlorella sorokiniana* MB-1. Bioresour Technol. 2018;262:74–9.
14. Niyogi KK, Bjrkman O, Grossman AR. The roles of specific xanthophylls in photoprotection. P Natl Acad Sci USA. 1998;94:14162–7.
15. Dall'Osto L, Lico C, Alric J, Giuliano G, Havaux M, Bassi R. Lutein is needed for efficient chlorophyll triplet quenching in the major LHCII antenna complex of higher plants and effective photoprotection in vivo under strong light. BMC Plant Biol. 2006. https://doi.org/10.1186/1471-2229-6-32.
16. Roth MS, Gallaher SD, Westcott DJ, Iwai M, Louie KB, Mueller M, Walter A, Foflonker F, Bowen BP, Ataii NN, et al. Regulation of oxygenic photosynthesis during trophic transitions in the green alga *Chromochloris zofingiensis*. Plant Cell. 2019;31:579–601.
17. Zhang Z, Sun DZ, Cheng KW, Chen F. Investigation of carbon and energy metabolic mechanism of mixotrophy in *Chromochloris zofingiensis*. Biotechnol Biofuels. 2021;14:36.
18. Choi WJ, Chae AN, Song KG, Park J, Lee BC. Effect of trophic conditions on microalga growth, nutrient removal, algal organic matter, and energy storage products in *Scenedesmus* (*Acutodesmus*) *obliquus* KGE-17 cultivation. Bioprocess Biosystems Eng. 2019;42:1225–34.
19. Tan L, Xu W, He X, Wang J. The feasibility of Fv/Fm on judging nutrient limitation of marine algae through indoor simulation and in situ experiment. Estuar Coast Shelf Sci. 2019;229: 106411.
20. Li X, Li W, Zhai J, Wei H, Wang Q. Effect of ammonium nitrogen on microalgal growth, biochemical composition and photosynthetic performance in mixotrophic cultivation. Bioresour Technol. 2019;273:368–76.
21. Ma R, Wang B, Chua ET, Zhao X, Chen J. Comprehensive utilization of marine microalgae for enhanced co-production of multiple compounds. Mar Drugs. 2020;18:467.
22. Takeshita T, Ota S, Yamazaki T, Hirata A, Zachleder V, Kawano S. Starch and lipid accumulation in eight strains of six *Chlorella* species under comparatively high light intensity and aeration culture conditions. Bioresour Technol. 2014;158:127–34.
23. Sun X, Cao Y, Xu H, Liu Y, Sun JR, Qiao DR, Cao Y. Effect of nitrogen-starvation, light intensity and iron on triacylglyceride/carbohydrate production and fatty acid profile of *Neochloris oleoabundans* HK-129 by a two-stage process. Bioresour Technol. 2014;155:204–12.
24. Levasseur W, Perre P, Pozzobon V. A review of high value-added molecules production by microalgae in light of the classification. Biotechnol Adv. 2020;41: 107545.
25. Pagliano C, Saracco G, Barber J. Structural, functional and auxiliary proteins of photosystem II. Photosynth Res. 2013;116:167–88.
26. Perez-Garcia O, Escalante FM, de-Bashan LE, Bashan Y. Heterotrophic cultures of microalgae: metabolism and potential products. Water Res. 2011;45:11–36.
27. Puzanskiy RK, Romanyuk DA, Shishova MF. Shift in expression of the genes of primary metabolism and chloroplast transporters in *Chlamydomonas reinhardtii* under different trophic conditions. Russ J Plant Physiol. 2020;67:867–78.
28. Morales-Sanchez D, Martinez-Rodriguez OA, Kyndt J, Martinez A. Heterotrophic growth of microalgae: metabolic aspects. World J Microbiol Biotechnol. 2015;31:1–9.
29. Wu T, Mao XM, Kou YP, Li YL, Sun H, He YJ, Chen F. Characterization of microalgal acetyl-CoA synthetases with high catalytic efficiency reveals their regulatory mechanism and lipid engineering potential. J Agric Food Chem. 2019;67:9569–78.
30. Boyle NR, Morgan JA. Flux balance analysis of primary metabolism in *Chlamydomonas reinhardtii*. BMC Syst Biol. 2009;3:4.
31. Zhang Y, Shi M, Mao X, Kou Y, Liu J. Time-resolved carotenoid profiling and transcriptomic analysis reveal mechanism of carotenogenesis

for astaxanthin synthesis in the oleaginous green alga *Chromochloris zofingiensis*. Biotechnol Biofuels. 2019;12:287.
32. Huang L, Gao B, Wu M, Wang F, Zhang C. Comparative transcriptome analysis of a long-time span two-step culture process reveals a potential mechanism for astaxanthin and biomass hyper-accumulation in *Haematococcus pluvialis* JNU35. Biotechnol Biofuels. 2019;12:18.
33. Reinfelder JR, Kraepiel AM, Morel FM. Unicellular C_4 photosynthesis in a marine diatom. Nature. 2000;407:996–9.
34. Bassham DC, Crespo JL. Autophagy in plants and algae. Front Plant Sci. 2014;5:679.
35. Tran QG, Yoon HR, Cho K, Lee SJ, Crespo JL, Ramanan R, Kim HSJC. Dynamic interactions between autophagosomes and lipid droplets in *Chlamydomonas reinhardtii*. Cells. 2019;8:992.
36. Wang XD, Song YN, Liu BL, Hang W, Li RJ, Cui HL, Li RZ, Jia XY. Enhancement of astaxanthin biosynthesis in *Haematococcus pluvialis* via inhibition of autophagy by 3-methyladenine under high light. Algal Res. 2020;50: 101991.
37. Perez-Perez ME, Couso I, Heredia-Martinez LG, Crespo JL. Monitoring autophagy in the model green microalga *Chlamydomonas reinhardtii*. Cells. 2017;6:36.
38. Nakatogawa H, Ichimura Y, Ohsumi Y. Atg8, a ubiquitin-like protein required for autophagosome formation, mediates membrane tethering and hemifusion. Cell. 2007;130:165–78.
39. Rathod JP, Vira C, Lali AM, Prakash G. Metabolic engineering of *Chlamydomonas reinhardtii* for enhanced beta-carotene and lutein production. Appl Biochem Biotechnol. 2020;190:1457–69.
40. Li M, Gan Z, Cui Y, Shi C, Shi X. Structure and function characterization of the phytoene desaturase related to the lutein biosynthesis in *Chlorella protothecoides* CS-41. Mol Biol Rep. 2013;40:3351–61.
41. Grunewald K, Eckert M, Hirschberg J, Hagen C. Phytoene desaturase is localized exclusively in the chloroplast and up-regulated at the mrna level during accumulation of secondary carotenoids in *Haematococcus pluvialis* (Volvocales, Chlorophyceae). J Plant Physiol. 2000;122:1261–8.
42. Galarza JI, Gimpel JA, Rojas V, Arredondo-Vega BO, Henriquez V. Over-accumulation of astaxanthin in *Haematococcus pluvialis* through chloroplast genetic engineering. Algal Res. 2018;31:291–7.
43. Deng YY, Cheng L, Wang Q, Ge ZH, Zheng H, Cao TJ, Lu QQ, Yang LE, Lu S. Functional characterization of lycopene cyclases illustrates the metabolic pathway toward lutein in red algal seaweeds. J Agric Food Chem. 2020;68:1354–63.
44. Liang MH, Xie H, Chen HH, Liang ZC, Jiang JG. Functional identification of two types of carotene hydroxylases from the green alga *Dunaliella bardawil* rich in lutein. Acs Synth Biol. 2020;9:1246–53.
45. Kim M, Kang J, Kang Y, Kang BS, Jin E. Loss of function in zeaxanthin epoxidase of *Dunaliella tertiolecta* caused by a single amino acid mutation within the substrate-binding site. Mar Drugs. 2018;16:418.
46. Liu J, Sun Z, Mao X, Gerken H, Wang X, Yang W. Multiomics analysis reveals a distinct mechanism of oleaginousness in the emerging model alga *Chromochloris zofingiensis*. Plant J. 2019;98:1060–77.
47. Paliwal C, Pancha I, Ghosh T, Maurya R, Chokshi K, Vamsi Bharadwaj SV, Ram S, Mishra S. Selective carotenoid accumulation by varying nutrient media and salinity in *Synechocystis* sp. CCNM 2501. Bioresour Technol. 2015;2015(197):363–8.
48. Ma RJ, Zhang Z, Ho SH, Ruan CX, Li J, Xie YP, Shi XG, Liu LM, Chen JF. Two-stage bioprocess for hyper-production of lutein from microalga *Chlorella sorokiniana* FZU60: effects of temperature, light intensity, and operation strategies. Algal Res. 2020;52: 102119.
49. Ma R, Zhao X, Ho SH, Shi X, Liu L, Xie Y, Chen J, Lu Y. Co-production of lutein and fatty acid in microalga *Chlamydomonas* sp. JSC4 in response to different temperatures with gene expression profiles. Algal Res. 2020;47: 101821.
50. Love MI, Huber W, Anders S. Moderated estimation of fold change and dispersion for RNA-seq data with DESeq2. Genome Biol. 2014;15:550.
51. Robinson MD, McCarthy DJ, Smyth GK. edgeR: a Bioconductor package for differential expression analysis of digital gene expression data. Bioinformatics. 2010;26:139–40.
52. Shi Y, Liu M, Ding W, Liu J. Novel insights into phosphorus deprivation boosted lipid synthesis in the marine alga *Nannochloropsis oceanica* without compromising biomass production. J Agric Food Chem. 2020;68:11488–502.
53. Azaman SNA, Wong DCJ, Tan SW, Yusoff FM, Nagao N, Yeap SK. De novo transcriptome analysis of *Chlorella sorokiniana*: effect of glucose assimilation, and moderate light intensity. Sci Rep. 2020;10:17331.

Publisher's Note